TUNGSTEN COATING APPLIED TO RADIOACTIVE WASTE CONTAINERS BY THE GAS-PHASE METHOD: ASSESSMENT OF CORROSION PROPERTIES

Dushik V. V., Abramova E. S., Shapagina N. A., Safonov A. V.

Federal State Budgetary Institution of Science A. N. Frumkin Institute of Physical Chemistry and Electrochemistry of the Russian Academy of Sciences, Moscow, Russia

Article received on February 1, 2024

The article summarizes the study exploring the anti-corrosion characteristics of tungsten coatings produced by chemical gas-phase deposition in a solution simulating the geochemical conditions at the Yeniseiskiy site. The study shows that a 30-micron-thick tungsten-based coating appears to be quite stable with an average corrosion rate of 1.4 microns/year. It also notes the high stability of tungsten coatings under microbial fouling conditions.

Keywords: *radioactive waste, metal containers, tungsten coating, anti-corrosion properties, microbial corrosion.*

Introduction

Corrosion of metals and alloys prompted by their exposure to the environment is seen as the main factor contributing to their degradation [1]. A most common method applied to protect the materials from the corrosion processes is the use of protective metal coatings, which, depending on their structure, promote various principles of anti-corrosion protection, including the barrier principle, when the base material is isolated from the effects produced by the destructive environment by a layer of a corrosion-resistant material. Elements such as nickel, chromium, zinc and cobalt are most often applied as such coatings. Degradation of metal equipment and containers with radioactive waste (RW) under extreme physical and chemical exposure is a problem studied in nuclear power engineering [2]. In other countries, thick-walled copper packages (Finland and Sweden) [3] and inhibiting, for example, nickel phosphide coatings [4] are applied to address the problems associated with the corrosion of metal containers with spent nuclear fuel (SNF). Stainless steels, titanium alloys and nickel-based alloys are used in France [5]. All of these have certain advantages and disadvantages, one of which often accounts for the high cost.

Currently, an underground radioactive waste repository is being developed in the Yenisei region (the Krasnoyarsk Territory, Russian Federation). According to its designs, steel containers with glass waste forms are going to be emplaced into purpose-designed boreholes and tunnels at a depth of 400—500 meters excavated in a crystalline rock mass. Under the operating conditions expected in such rock repositories, elevated temperatures (45—90 °C) and absence of oxygen in the corrosive environment are possible. When moisture ingress occurs, chemical and electrochemical reactions with oxygen depolarization may evolve, which may reduce considerably the service life of metal container materials, as well as the microbial-induced corrosion processes [6]. Decision-making on the method to be implemented to protect the packaging from complex degradation under elevated temperatures is a non-trivial task, since it involves not only searching for a corrosion-resistant coating, but also forecasting the service life of this material

over quite a long-time period, i.e. over 10,000 years. Tungsten is the heaviest and most refractory metal and therefore is mainly applied in the industry as a heat-resistant and heat-proof protective material in electronic vacuum devices [7], [8], high-temperature thermocouples [9], as well as plasma-facing elements in thermonuclear fusion plants and has some other applications in the fuel and energy complex [9]—[15]. Heat-resistant alloys and high-speed steels containing tungsten, as well as hard alloys with tungsten carbide, are well known [7]. However, modern production methods enable the use of tungsten and its alloys as independent anticorrosive materials and coatings with some unique characteristics. They can be obtained by chemical vapor deposition [16], [17] on copper, nickel [18] and steel substrates through a supporting layer of nickel obtained by deposition from solutions [19]—[21]. For this reason, it is of interest to consider the anticorrosive properties of new coatings that can be potentially applied to protect the materials of containers or secondary packages (canisters) designed for RW disposal. This article studies their characteristics under microbiological corrosion conditions.

Methodology and materials

Tungsten coating production. Tungsten coatings were produced by chemical vapor deposition from tungsten hexafluoride and hydrogen mixture on copper plates using a chemical vapor deposition unit (Figure 1). The chemical process enabling tungsten synthesis from its fluoride can be described by the following reaction:

$$WF_6 + 3H_2 = W + 6HF.$$

Tungsten hexafluoride (3 l/h) and hydrogen (10 l/h) fed from vessels were supplied through gas flow regulators to a vacuum chemical reactor with a hot wall, where the tungsten deposition process evolved on a surface heated to 550 °C at a total pressure of 50 mm Hg provided by a vacuum pump and lasted for 2 hours. The reaction products were fed into a cryogenic trap and subsequently neutralized with a weakly alkaline solution. Copper grade M1 was used as a substrate material.

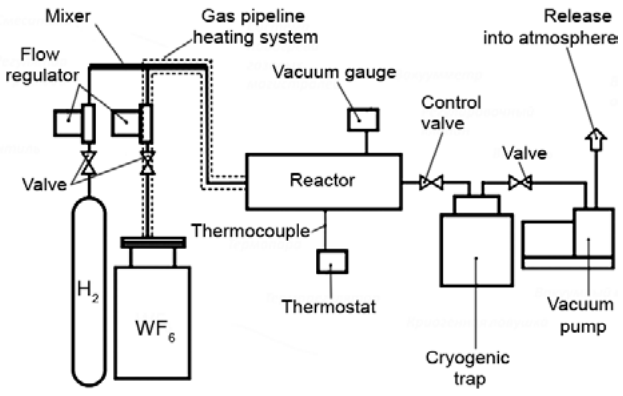

Figure 1. Flowchart describing the chemical vapor deposition of tungsten

The coating thickness was measured by optical microscopy using the PMT-3M microhardness measuring system based on a transverse section of witness samples processed under the same process.

Corrosion experiments. Rectangular copper plates M1 of 10×15×1 mm with a tungsten coating were used to study the corrosion processes. Before launching the experiment, the samples were washed in an ultrasonic bath Sapphire-0.8 TC (Russia) in a mixture of $C_2H_5OH : C_7H_8 = 1 : 1$ for 25 minutes.

Sterile 200 ml glass vials were filled with 50 ml of sterile model water (SMW) containing (mg/l) $NaHCO_3$ — 272, $CaCl_2$ — 71.8, $MgSO_4 \cdot 7H_2O$ — 70, pH 7.1 and simulating the composition of formation waters inherent in the Yeniseiskiy site [22]. The plate samples were suspended in the medium, after which the vials were sealed hermetically, evacuated in an ultrasonic bath, and then argon was added to the gas phase to establish anaerobic conditions.

To assess the microbiological factor as regards its contribution to corrosion, an accumulative culture of underground biota inherent in the formation waters sampled directly from the Yeniseiskiy site was introduced into the liquid phase. The microorganisms and their characteristics were discussed in [6]. Glucose was introduced at a concentration of 500 mg/l to stimulate growth.

The corrosion rate was assessed gravimetrically. A dilute solution of hydrofluoric acid was used to remove its products: 500 ml of HF was added to 500 ml of water. The etching process lasted for 3 minutes at room temperature.

The corrosion rate of the samples (μm/year) was calculated based on the below formula (1):

$$V_{cor} = \Delta m \cdot 8760/(S \cdot t \cdot \rho), \quad (1)$$

where Δm is the average mass difference of the samples before/after testing, g; S is the metal surface area, m^2; t is the testing time, h; ρ is the metal density, g/cm^3.

The average area of corrosion damage was calculated based on the appearance of the tungsten coating after a 120-day testing using the CamRec-009 2D software (TechSmith, USA).

Chemical composition of the surface layers formed on the metals during their exposure to corrosive environments was evaluated based on X-ray photoelectron spectroscopy (XPS). The XPS spectra obtained for the surface layers were recorded on an OMICRON ESCA+ device (OMICRON, Germany).

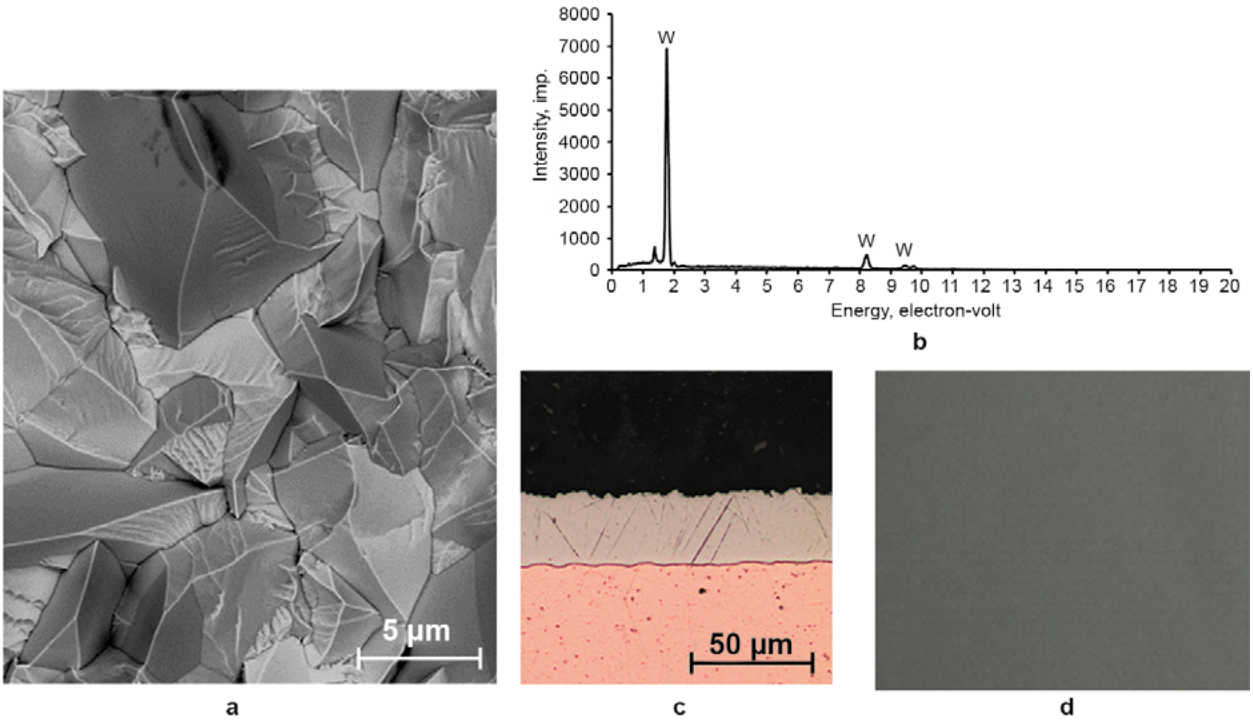

Figure 2. Tungsten coating produced by chemical vapor deposition: a) electron microscopic image of morphology; b) energy-dispersive X-ray spectrum from the surface; c) optical image of a cross-section; d) photograph of the surface

The pressure in the analyzer chamber was maintained at a level of no higher than $8 \cdot 10^{-10}$ mbar, the Al anode was applied as a source of AlK_α radiation (hν = 1486.6 eV). The analyzer transmission energy accounted for 20 eV. To account for the sample charging, XPS peaks were standardized according to their position relative to the maximum of C1s hydrocarbon contaminants (E_b = 285.0 eV). The spectra were decomposed into components in the UNIFIT 2009 software. The background was calculated based on the Shirley method.

Results and discussion

Characteristics of the tungsten coating

Figure 2 shows the appearance and composition of the coating obtained based on chemical vapor deposition.

The coating has a fairly developed morphology (Figure 2a) associated with a columnar structure typical of CVD (chemical vapor deposition) coatings, tungsten accounts for its only component (Figure 2b). The size of the structural elements is estimated at about 5 μm, which is comparable to the transverse dimension of the columnar tungsten grain obtained in this mode. Such a structure, given its application as an anti-corrosion agent, can be viewed as a negative factor, since it may result in through holes evolving in the inter-crystalline areas. Nevertheless, in the initial state (Figure 2c), such porosity is absent, which seems a favorable factor considering the corrosion-protective properties of the coating having a uniform gray color and a matte surface (Figure 2d) due to its roughness.

Results of corrosion tests

Figure 3 shows the results of corrosion tests with tungsten samples that were exposed to different environments for 120 days. In all cases, no foci of local metal dissolution were recorded on the surface, nevertheless general etching of tungsten was detected (Figure 3, MW). In case of microbial action

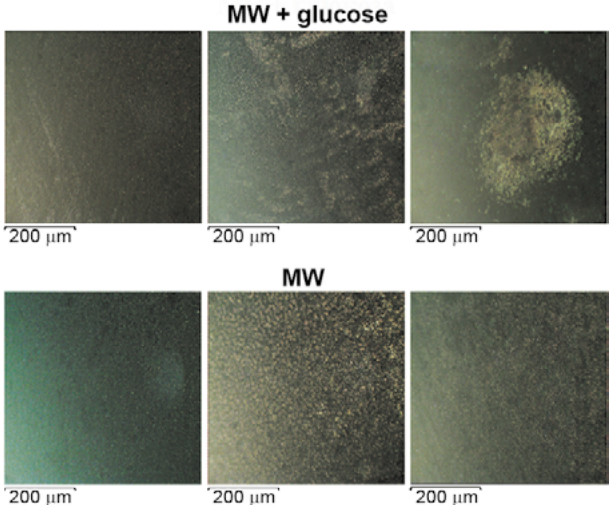

Figure 3. Microphotographs of the W surface after having been exposed for 120 days in solutions: MW (model water, control sample), MW+glucose (model water with some added microorganisms)

(Figure 3, MW + glucose), areas covered and uncovered with corrosion products were identified on the surface.

Figure 4 and Table 1 present the gravimetric studies that showed that the average corrosion rate for the tungsten coating in low-mineralized MW was 1.4 μm/year, while given the microbial action, it grew up to 3.8 μm/year. The average area of corrosion damage in the MW of the Yeniseiskiy site accounted for (7.0 ± 0.4) %, i. e., based on the appearance of the tungsten coating subjected to a 120-day testing, in case of microbial exposure this indicator amounted to (12.0 ± 0.7) %.

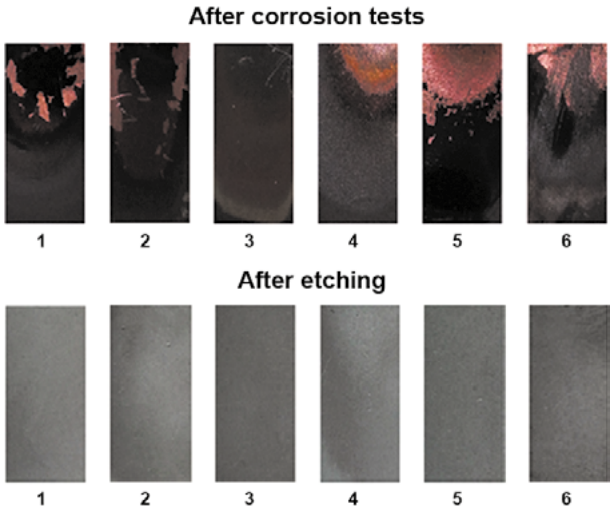

Figure 4. Appearance of tungsten coating upon completing the corrosion tests on day 120 and after etching: MW+glucose (model water with some added microorganisms) – samples 1–3, MW (model water, control sample) – samples 4–6

Table 1. Corrosion rates measured for the tungsten coatings of the samples

№	Donor	V_{cor}, μm/year	$V_{cor\ av}$, μm/year	Average area of corrosion damage, %
1	MW + glucose	5.02	3.8	12.0 ± 0.7
2		3.85		
3		2.47		
4	MW	1.02	1.4	7.0 ± 0.4
5		1.85		
6		1.47		

Evaluation of the sample surface by the XPS method

According to the XPS studies, a few tungsten states could be observed on the sample surface before the corrosion tests were launched, which can

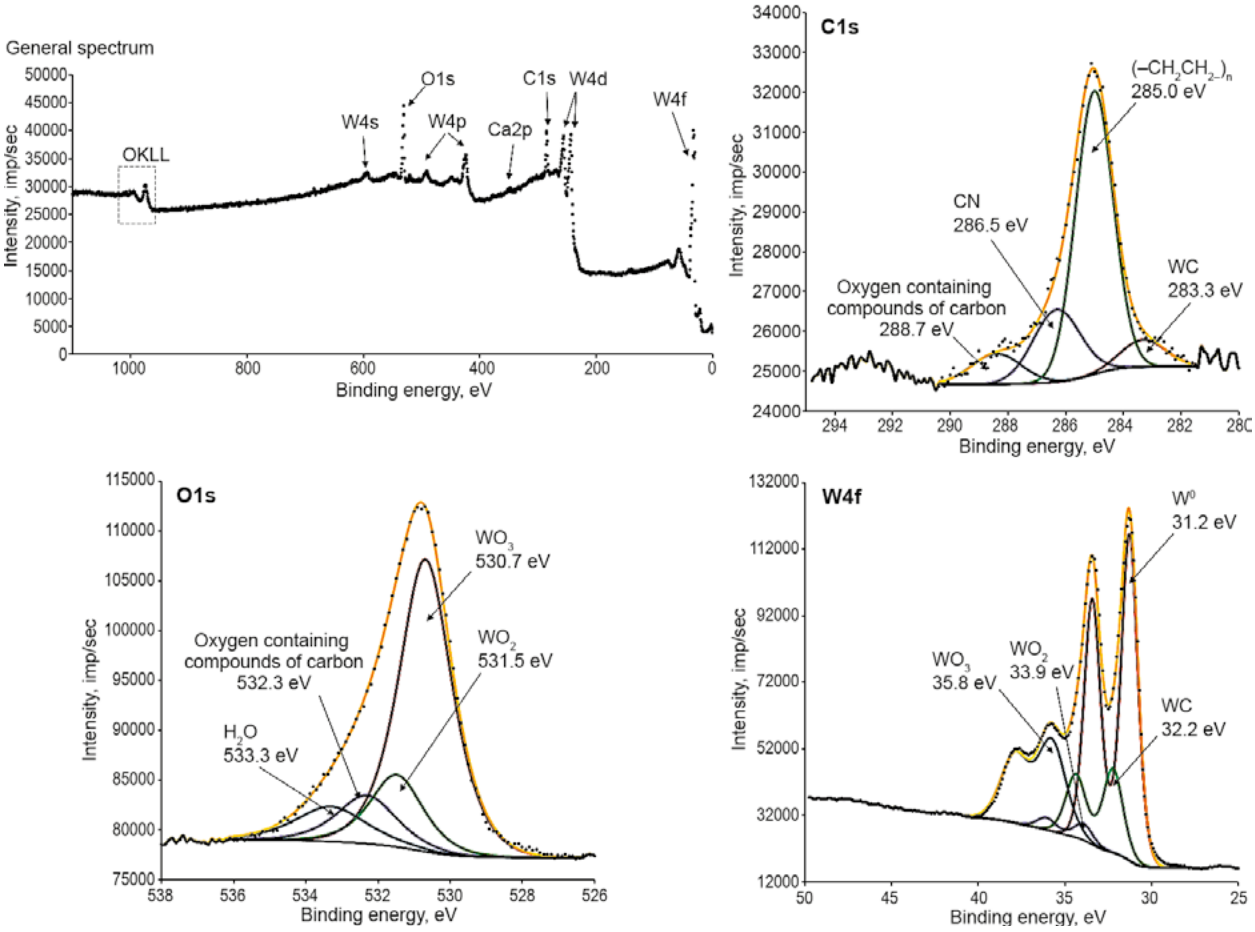

Figure 5. XPS spectra of tungsten surface

be correlated by the binding energy with metallic W^0 (31.2 eV), carbide (32.2 eV) and oxides — WO_2 (33.9 eV) and WO_3 (35.8 eV) (Figure 5). The last two states were also confirmed by the O1s and C1s spectra involving peaks for O1s — WO_3 (529.8 eV) and WO_2 (530.9 eV), and WC (283.3 eV) for C1s.

At the post-corrosion stage, the overview spectra of the samples, while maintaining the main lines inherent in the main element and in addition to increased surface contamination, showed some lines characteristic of copper, aluminum and sulfur, the spectrum of which can be decomposed into three doublets as it comes to the sample with microorganisms related to WS_2 (161.4 eV), Cu_2S (162.4 eV) and CS_2 (163.5 eV), and two doublets — WS_2 and CS_2 — with similar binding energies. In this case, the tungsten spectrum W4f also changes: the metallic state was not detected, but additional states WS2 with a binding energy of 32.3 eV and tungstates (37.5 eV) were nevertheless observed. The oxygen spectrum O1s also showed an influx in the region of lower binding energies, which could be compensated by the peak of 529.9 eV and related to $Me^{n+}(WO_4)_n$. Phosphorus was not detected in the samples.

Conclusion

A 30-μm-thick tungsten coating was applied to a copper substrate via the gas-phase deposition method at tungsten hexafluoride and hydrogen flow rates of 3 l/h and at 10 l/h respectively, a pressure of 50 mm Hg and a temperature of 550 °C. This coating appears to be quite stable under the model conditions expected at the Yeniseiskiy site with an average corrosion rate of 1.4 μm/year. As it comes to the general nature of the corrosion dissolution process specific for such coatings, one should note that it has no local foci, which is an important difference compared to other materials. According to the XPS spectroscopy data, copper reflections, which is the substrate substance, were absent on the tungsten surface following 120 days of exposure, which indicates the low porosity of these coatings and high efficiency of material shielding from the corrosive environment and its exposure. It should be added that the corrosion product of tungsten is WO_3, which, in the pH range of 5—8, is much more inert compared to metallic tungsten, iron and copper oxides. It is important to note relatively high stability of tungsten coatings under microbial fouling conditions. Under intensive microflora development, a twofold increase in the corrosion rate was noted compared to St3 steel, for which a 5—10-fold increase had been noted previously [23]. The chemical vapor deposition method enables tungsten application to products of various configurations, including RW storage containers made of both copper and low-alloy steel. The cost estimated assuming a 100-micron-thick tungsten coating applied on the entire area of the inner surface of a 200-liter container amounted to some 150 thousand rubles, and, taking into account the anti-corrosion effectiveness of the coating, this approach can be considered economically feasible.

References

1. Iannuzzi M., Frankel G. S. The carbon footprint of steel corrosion. *Npj Materials Degradation,* 2022, vol. 6 (1), p. 101. DOI: 10.1038/s41529-022-00318-1.

2. Kryuchkov D. V., Boldyrev K. A. Printsipy kompleksnogo ucheta protsessov ehvolyutsii inzhenernykh bar'erov bezopasnosti pri otsenke rasprostraneniya radionuklidov za predely ob"ekta [Principles Ensuring Comprehensive Accounting of Processes Associated with Engineered Safety Barriers' Evolution: Assessing Radionuclide Spread Beyond Site Boundaries]. *Radioaktivnye otkhody — Radioactive Waste,* 2019, no. 4 (9), pp. 106—115. DOI: 10.25283/2587-9707-2019-4-106-115.

3. King F., Lilja C., Pedersen K., Pitkaenen P., Vaehaenen M. *An update of the state-of-the-art report on the corrosion of copper under expected conditions in a deep geologic repository* (SKB-TR-10-67). Sweden, 2010.

4. Deyab M. A., Ouarsal R., Lachkar M., El Bali B., Essehli R. Phosphites compound: Novel corrosion inhibitor for radioactive waste container (carbon steel) in simulated Callovo-Oxfordian (COx) groundwater. *Journal of Molecular Liquids,* 2016, vol. 219, pp. 994—999. DOI: 10.1016/j.molliq.2016.04.027.

5. King F. Container Materials for the Storage and Disposal of Nuclear Waste. *Corrosion,* 2013, vol. 69, no. 10, pp. 986—1011. DOI: 10.5006/0894.

6. Abramova E., Popova N., Artemiev G., Boldyrev K., Kazakov K., Kryuchkov D., Safonov A. Biological factors affecting the evolution of safety barrier materials in the Yeniseisky deep geological repository. *Engineering Geology,* 2023, vol. 312, p. 106931. DOI: 10.1016/j.enggeo.2022.106931.

7. Zelikman A. N., Nikitina L. S. *Vol'fram* [Tungsten]. Moscow, Metallurgiya Publ., 1978. 272 p.

8. Lassner E., Schubert W.-D. *Tungsten: Properties, chemistry, technology of the element, alloys, and chemical compounds.* Springer, 1999. 422 p.

9. Kim H., Lee H. J., Kim S. H., Jang C. Plasma thermal performance of a dual-process PVD/PS tungsten coating on carbon-based panels for nuclear fusion application. *Fusion Engineering and Design,* 2016, vol. 109—111. Part A. Pp. 590—595. DOI: 10.1016/j.fusengdes.2016.02.040.

10. García Gallardo J. A., Giménez M. A. N., Gervasoni J. L. Nuclear properties of Tungsten under 14 MeV neutron irradiation for fusion-fission hybrid reactors. *Annals of Nuclear Energy,* 2020, vol. 147, p. 107739. DOI: 10.1016/j.anucene.2020.107739.
11. Xie J., Lu H., Lu J., Song X., Wu Sh., Lei J. Additive manufacturing of tungsten using directed energy deposition for potential nuclear fusion application. *Surface and Coatings Technology,* 2021, vol. 409, p. 126884. DOI: 10.1016/j.surfcoat.2021.126884.
12. Pitts R. A. et al. Physics basis for the first ITER tungsten divertor. *Nuclear Materials and Energy,* 2019, vol. 20, p. 100696. DOI: 10.1016/j.nme.2019.100696.
13. Bachmann C. et al. Issues and strategies for DEMO in-vessel component integration. *Fusion Engineering and Design,* 2016, vol. 112, pp. 527—534. DOI: 10.1016/j.fusengdes.2016.05.040.
14. Harutyunyan Z., Ogorodnikova O., Gasparyan Y., Efimov V., Sorokin I., Sergeev N. et al. Tungsten fuzz annealing effect on deuterium retention in polycrystalline tungsten. *Journal of Nuclear Materials,* 2022, vol. 567, p. 153811. DOI: 10.1016/j.jnucmat.2022.153811.
15. Zalavutdinov R., Novokhatsky A., Gusev V. et al. Electron beam treatment of tungsten mock-ups. *Physica Scripta,* 2017, vol. 2017, no. T170, p. 014043. DOI: 10.1088/1402-4896/aa8b00.
16. Krasovskiy A. I., Chuzhko R. K., Balakhovskiy O. A., Tregulov V. R. *Ftoridnyy protsess polucheniya vol'frama. Fiziko-khimicheskiye osnovy. Svoystva metalla* [Tungsten production by the fluoride process. Physical and chemical fundamentals. Properties of metal]. Moscow, Nauka Publ., 1981. 261 p.
17. Korolev Yu. M., Stolyarov V. I. *Vosstanovleniye ftoridov tugoplavkikh metallov vodorodom* [Fluorides from refractory metals reduced by hydrogen]. Moscow, Metallurgiya Publ., 1981. 184 p.
18. Dushik V. V., Rozhanskii N. V., Lifshits V. O. et al. The formation of tungsten and tungsten carbides by CVD synthesis and the proposed mechanism of chemical transformations and crystallization processes. *Materials Letters,* 2018, vol. 228, pp. 164—167. DOI: 10.1016/j.matlet.2018.06.003.
19. Dushik V. V., Ruban E. A., Drovosekov A. B. et al. Synergetic Effect in Ni-P-W and W-C Multilayer Coating Systems Obtained by Chemical-Catalytic Metallization and Chemical-Vapor Deposition. *Journal of Surface Investigation: X-ray, Synchrotron and Neutron Techniques,* 2023, vol. 17, pp. 1364—1371. DOI: 10.1134/S1027451023060265.
20. Dushik V. V., Ruban E. A., Shaporenkov A. A. et al. Mechanical Properties and Corrosion-Electrochemical Behavior of Multilayer Coatings of the Ni-P and W-C Systems Obtained by Chemical-Catalytic Metallization and Chemical Vapor Deposition. Part 1: Structure and Mechanical Properties of Coatings. *Protection of Metals and Physical Chemistry of Surfaces,* 2022, vol. 58, no. 7, pp. 1301—1306. DOI: 10.1134/S2070205122070048.
21. Dushik V. V., Levdikova K. S., Shaporenkov A. A. et al. Mekhanicheskiye svoystva i korrozionno-elektrokhimicheskoye povedeniye mnogosloynykh pokrytiy sistemy Ni-P i W-C, poluchayemykh metodami khimiko-kataliticheskoy metallizatsii i khimicheskogo gazofaznogo osazhdeniya. Chast' 2: Korrozionno-elektrokhimicheskoye povedeniye pokrytiy [Mechanical Properties and Corrosion-Electrochemical Behavior of Multilayer Coatings of Ni-P and W-C Systems, Obtained by Methods of Electoless Plating and Chemical Vapor Deposition. Part 2. Corrosion and Electrochemical Behavior of Coatings]. *Korroziya: materialy, zashchita — Corrosion: materials, protection,* 2022, no. 2, pp. 43—48. DOI: 10.31044/1813-7016-2022-0-2-43-48.
22. Rozov K. B., Rumynin V. G., Nikulenkov A. M., Leskova P. G. Sorption of ^{137}Cs, ^{90}Sr, Se, ^{99}Tc, $^{152(154)}$Eu, $^{239(240)}$Pu on fractured rocks of the Yeniseysky site (Nizhne-Kansky massif, Krasnoyarsk region, Russia). *Journal of Environmental Radioactivity,* 2018, vol. 192, pp. 513—523. DOI: 10.1016/j.jenvrad.2018.08.001.
23. Boldyrev K. A., Safonov A. V., Abramova E. S., Gladkikh N. A., Kryuchkov D. V. Issledovanie korrozii uglerodistoi stali St3 v prisutstvii mikroorganizmov, vydelennykh iz podzemnykh vod na uchastke "Eniseiskii" [Research on the St3 Carbon Steel Corrosion in the Presence of Microorganisms Isolated from the Groundwater at the Yeniseyskiy Site]. *Radioaktivnye otkhody — Radioactive Waste,* 2021, no. 3 (16), pp. 103—113. DOI: 10.25283/2587-9707-2021-3-103-113.

Information about the authors

Dushik Vladimir Vladimirovich, PhD in Chemical Sciences, Leading Researcher, Federal State Budgetary Institution of Science A. N. Frumkin Institute of Physical chemistry and Electrochemistry of the Russian Academy of Sciences (31, bld. 4, Leninsky prospect, Moscow, 119071, Russia), e-mail: v.dushik@gmail.com.

Abramova Elena Sergeevna, engineer of the 1st category, Federal State Budgetary Institution of Science A. N. Frumkin Institute of Physical chemistry and Electrochemistry of the Russian Academy of Sciences (31, bld. 4, Leninsky prospect, Moscow, 119071, Russia), e-mail: gorchicta246@mail.ru.

Shapagina Natalia Andreevna, PhD in Chemical Sciences, Senior Researcher, Federal State Budgetary Institution of Science A. N. Frumkin Institute of Physical chemistry and Electrochemistry of the Russian Academy of Sciences (31, bld. 4, Leninsky prospect, Moscow, 119071, Russia), e-mail: fuchsia32@bk.ru.

Safonov Aleksej Vladimirovich, PhD in Chemical Sciences, Leading Researcher, Federal State Budgetary Institution of Science A. N. Frumkin Institute of Physical chemistry and Electrochemistry of the Russian Academy of Sciences (31, bld. 4, Leninsky prospect, Moscow, 119071, Russia), e-mail: alexeysafonof@gmail com.

Bibliographic description

Dushik V. V., Abramova E. S., Shapagina N. A., Safonov A. V. Tungsten Coating Applied to Radioactive Waste Containers by the Gas-Phase Method: Assessment of Corrosion Properties. *Radioactive Waste,* 2024, no. 2 (27), pp. 50—58. DOI: 10.25283/2587-9707-2024-2-50-58. (In Russian).